BJP BRITISH JOURNAL OF PHARMACOLOGY
BPS BRITISH PHARMACOLOGICAL SOCIETY

BJP British Journal of Pharmacology

DOI:10.1111/j.1476-5381.2010.01026.x
www.brjpharmacol.org

RESEARCH PAPER

Mechanisms of actions of hydrogen sulphide on rat distal colonic epithelium

E Pouokam and M Diener

Institute for Veterinary Physiology, Justus-Liebig-University Giessen, Giessen, Germany

Correspondence
M. Diener, Institut für Veterinär-Physiologie, Justus-Liebig-Universität Gießen, Frankfurter Str. 100, D-35392 Gießen, Germany. E-mail: martin.diener@vetmed.uni-giessen.de

Keywords
Ca^{2+} signalling; Cl^- secretion; electrolyte transport; NaHS; rat colon

Received
18 May 2010
Revised
16 August 2010
Accepted
23 August 2010

BACKGROUND AND PURPOSE
The aim of this study was to clarify the mechanisms by which hydrogen sulphide (H_2S) affects ion secretion across rat distal colonic epithelium.

EXPERIMENTAL APPROACH
Changes in short-circuit current induced by the H_2S-donor, sodium hydrosulphide (NaHS; 10 mmol·L^{-1}), were measured in Ussing chambers after permeabilization of the apical membrane with nystatin. Cytosolic Ca^{2+} concentration ($[Ca^{2+}]_i$) and Ca^{2+} in intracellular stores were measured with fluorescent dyes. Changes in mitochondrial membrane potential were estimated with rhodamine 123.

KEY RESULTS
NaHS had a biphasic effect on overall currents across the basolateral membrane: an initial inhibition followed by a secondary stimulation. Both a scilliroside-sensitive action on the Na^+-K^+-ATPase and modulation of glibenclamide-sensitive and tetrapentylammonium-sensitive (i.e. ATP-sensitive and Ca^{2+}-dependent) basolateral K^+ channels were involved in this action. Experiments with rhodamine 123 revealed that NaHS induced a hyperpolarization of the mitochondrial membrane. NaHS evoked a biphasic change in $[Ca^{2+}]_i$, an initial decrease followed by a secondary increase, known to be mediated by the release of stored Ca^{2+}. Initial falls in $[Ca^{2+}]_i$ were not mediated by a sequestration of Ca^{2+} in intracellular Ca^{2+} storing organelles, as the Mag-Fura-2 signal was unaffected by NaHS. Falls in $[Ca^{2+}]_i$ were inhibited by 2′,4′-dichlorobenzamil, an inhibitor of the Na^+-Ca^{2+}-exchanger, and attenuated in Na^+-free buffer, suggesting a transient stimulation of Ca^{2+} outflow by this transporter, directly demonstrated by Mn^{2+} quenching experiments.

CONCLUSIONS AND IMPLICATIONS
ATP-sensitive and Ca^{2+}-dependent basolateral K^+ conductances, the basolateral Na^+-K^+-pump as well as Ca^{2+} transporters were involved in the action of H_2S in regulating colonic ion secretion.

Abbreviations
$[Ca^{2+}]_I$, cytosolic Ca^{2+} concentration; Gt, tissue conductance; Isc, short-circuit current; TPeA, tetrapentylammonium

Introduction

Intestinal ion transport, which can be switched from absorption into secretion of water and electrolytes (see Binder and Sandle, 1994), is not only controlled by classical neurotransmitters or hormones, but also by the so-called 'gaso-transmitters'. Besides nitric oxide, the prototype of this class of volatile messenger molecules, more recently hydrogen sulphide (H_2S), has been recognized and identified as a transmitter. This gas is produced from cysteine via the enzymes cystathionine-β-synthase and cystathionine-γ-lyase (Wang, 2002). In the circulation, H_2S is known as a gaso-transmitter inducing vasodilatation, decreasing cardiac inotropy, and inhibiting the proliferation of vascular smooth

muscle (see Geng *et al.*, 2007; Lefer, 2008). Furthermore, H_2S donors have been shown to protect against burn- and smoke-induced acute lung injury in sheep (Esechie *et al.*, 2009) and to exert antiinflammatory actions in a model of rat synovitis (Ekundi-Valentim *et al.*, 2010).

In the intestine, a seminal observation in this field was the finding that enteric neurons express the key enzymes for H_2S production and that H_2S releasing drugs induce Cl^- secretion in guinea pig and human colon via excitation of submucosal secretomotor neurons. Neuronal capsaicin-sensitive cation channels, that is, transient receptor potential vanilloid receptor type 1 (TRPV1) channels are thought to be the primary target of H_2S in these two species (Schicho *et al.*, 2006; receptor and channel nomenclature follows Alexander *et al.*, 2009).

In contrast, in rat colonic epithelium, where H_2S also induces a Cl^- secretion, the neurotoxin, tetrodotoxin, only partially reduced the response in short-circuit current (Isc), a measure of net charge movement across the epithelium, which was induced by sodium hydrosulphide (NaHS), an H_2S donor (Lee *et al.*, 2006), indicating additional epithelial sites of action (Hennig and Diener, 2009). Furthermore, cystathionine-β-synthase and cystathionine-γ-lyase immunoreactivity were found within the colonic epithelium itself and isolated colonic crypts responded with changes in the cytosolic Ca^{2+} concentration ($[Ca^{2+}]_i$) in the presence of NaHS. The Isc response induced by NaHS was triphasic: an initial rise in Isc (mediated by Cl^- secretion) was followed by a transient fall (assumed to represent a transient K^+ secretion), before the Isc finally rose again to a long-lasting Cl^- secretory response. Also, the Ca^{2+} response was not monophasic; it consisted of a transient decrease of $[Ca^{2+}]_i$ followed by a long-lasting increase mediated by a release of stored Ca^{2+} via intracellular Ca^{2+} channels. The Cl^- secretory response was sensitive to serosal administration of glibenclamide, a known inhibitor of ATP-sensitive K^+ channels (see Cook and Quast, 1990), as well as tetrapentylammonium, known as an inhibitor of Ca^{2+}-dependent K^+ channels (Maguire *et al.*, 1999). This suggests that, as in smooth muscle cells from rat aorta (Zhao *et al.*, 2001) or rat insulinoma cells (Yang *et al.*, 2005), NaHS stimulates both ATP-sensitive K^+ channels and Ca^{2+}-dependent K^+ channels, which would be consistent with the observed increase in the cytosolic Ca^{2+} concentration, measured in isolated rat colonic crypts (Hennig and Diener, 2009).

In order to secrete Cl^- across the apical membrane, the basolateral membrane has to establish the driving force for anion extrusion via anion channels in the apical membrane. In the basolateral membrane, K^+ channels generate the driving force for Cl^- secretion by maintaining the negative membrane potential, which is dominated by a K^+ diffusion potential (Strabel and Diener, 1995; Warth and Barhanin, 2003), whereas the Na^+-K^+-ATPase has to maintain the K^+ concentration gradient between the intra- and the extracellular space as prerequisite for the establishment of the K^+ diffusion potential. In view of the extensive evidence for the stimulation of ATP-sensitive K^+ channels by H_2S (see above), it seemed to be of primary interest to investigate potential effects of NaHS on the basolateral membrane which dominates cellular K^+ conductance of the epithelium. The second question to be clarified was the identification of the mechanism involved in the early response of the cytosolic Ca^{2+} concentration, which is transiently decreased by NaHS, before the secondary release of stored Ca^{2+} begins. To this end, changes in Isc induced by the H_2S-donor, NaHS, were measured in Ussing chambers after permeabilization of the apical membrane with nystatin. This ionophore forms pores in the apical membrane and thereby bypasses this membrane. Consequently, all changes in Isc induced by NaHS can only result from changes in ion transport across the non-permeabilized basolateral membrane (Schultheiss and Diener, 1997). Changes of the cytosolic Ca^{2+} concentration were evaluated using Fura-2; the Ca^{2+} concentration in intracellular stores was measured with Mag-Fura-2; and changes in mitochondrial membrane potential were estimated with rhodamine 123.

Methods

Solutions

The standard solution for the Ussing chamber experiments was a buffer solution containing ($mmol \cdot L^{-1}$): NaCl 107, KCl 4.5, $NaHCO_3$ 25, Na_2HPO_4 1.8, NaH_2PO_4 0.2, $CaCl_2$ 1.25, $MgSO_4$ 1 and glucose 12. The solution was gassed with carbogen (5% CO_2 in 95% O_2, v/v); pH was 7.4. In order to apply a K^+ gradient, the KCl concentration in this buffer was increased to 13.5 $mmol \cdot L^{-1}$ at the mucosal side while reducing the NaCl concentration in order to maintain isoosmolarity. For the Na^+-free solution, NaCl was replaced by N-methyl-D-glucamine ($NMDG^+$) chloride.

For the experiments carried out with isolated crypts, the following buffers were used. The EDTA solution for the isolation contained ($mmol \cdot L^{-1}$): NaCl 107, KCl 4.5, $NaHCO_3$ 25, Na_2HPO_4 1.8, NaH_2PO_4 0.2, glucose 12.2, EDTA 10 and 1 $g \cdot L^{-1}$ bovine serum albumin (BSA). It was gassed with carbogen; pH was adjusted by Tris-base to 7.4. The

isolated crypts were stored in a high potassium Tyrode solution consisting of (mmol·L^{-1}): K gluconate 100, KCl 30, HEPES 10, NaCl 20, $MgCl_2$ 1, $CaCl_2$ 1.25, glucose 12.2, sodium pyruvate 5 and 1 g·L^{-1} BSA; pH was 7.4. For superfusion of the isolated crypts during the imaging experiments, the following buffer was used (in mmol·L^{-1}): NaCl 140, KCl 5.4, $CaCl_2$ 1.25, $MgSO_4$ 1, HEPES 10, glucose 12.2; pH was 7.4. For the Na^+-free Tyrode solution, NaCl was replaced by NMDG Cl.

Tissue preparation and crypt isolation

All animal care and experimental procedures were approved by Regierungspräsidium Gießen, Gießen, Germany. Wistar rats of both sexes were used with a weight of 180–240 g. The animals had free access to water and a standard rat diet until the day of the experiment. Animals were killed by stunning followed by exsanguination. The serosa and muscularis propria were stripped away to obtain a mucosa-submucosa preparation of the distal colon. The distal colon was distinguished from the proximal colon by the absence of palm leaf-like striae (Lindström *et al.*, 1979). Briefly, the colon was placed on a small plastic rod with a diameter of 5 mm. A circular incision was made near the anal end with a blunt scalpel, and the serosa together with the lamina propria was gently removed in a proximal direction. Two segments of the distal colon of each rat were prepared. In general, one tissue served to measure the control response evoked by NaHS and the other was treated with putative antagonists before NaHS was applied. If the antagonist had to be administered in a solvent, the control tissue was pretreated with that solvent.

For the isolation of intact crypts, the mucosa-submucosa was fixed on a plastic holder with tissue adhesive and transferred for about 7 min to the EDTA solution. The mucosa was vibrated once for 30 s in order to obtain crypts (Schultheiss *et al.*, 2002). They were collected in a high-K^+ gluconate Tyrode buffer.

Isc measurement

The mucosa–submucosa preparation was fixed in a modified Ussing chamber, bathed with a volume of 3.5 mL on each side of the mucosa. The tissue was incubated at 37°C and short-circuited by a computer-controlled voltage-clamp device (Ingenieur Büro für Mess- und Datentechnik Mussler, Aachen, Germany) with correction for solution resistance. Tissue conductance was measured every minute by the voltage deviation induced by a current pulse (±50 µA, duration 200 ms) under open-circuit conditions. Isc was continuously recorded on a chart recorder. Isc is expressed as µEq·h^{-1}·cm^{-2}, that is, the flux of a monovalent ion per time and area, with 1 µEq·h^{-1}·cm^{-2} = 26.9 µA·cm^{-2}.

Imaging experiments

Relative changes in the cytosolic Ca^{2+} concentration were measured using Fura-2 (Molecular Probes, Leiden, the Netherlands), a Ca^{2+}-sensitive fluorescent dye (Grynkiewicz *et al.*, 1985). The crypts were pipetted into the experimental chamber with a volume of about 3 mL. They were attached to the glass bottom of the chamber with the aid of poly-L-lysine (0.1 g·L^{-1}; Biochrom, Berlin, Germany). The crypts were incubated for 60 min with 2.5 µmol·L^{-1} Fura-2 acetoxymethylester (AM). Then the dye ester not taken up by the cells was washed away. The preparation was superfused hydrostatically throughout the experiment with 140 mmol·L^{-1} NaCl Tyrode. Perfusion rate was about 1 mL·min^{-1}.

Changes in the cytosolic Ca^{2+} concentration were monitored as changes in the Fura-2 ratio (R; emission at an excitation wave length of 340 nm divided by the emission at an excitation wave length of 380 nm). Experiments were carried out on an inverted microscope (Olympus IX-50; Olympus, Hamburg, Germany), equipped with an epifluorescence set-up and an image analysis system (Till Photonics, Martinsried, Germany). Several regions of interest, each with the size of about one cell, were placed over an individual crypt. The emission above 420 nm was measured from the regions of interest. Data were sampled at 0.2 Hz. The baseline in the fluorescence ratio of Fura-2 was measured for several minutes before drugs were administered. For the Mn^{2+} quench experiments, the Fura-2 fluorescence was measured at a single wavelength, 360 nm, i.e. the isoemissive wavelength of this dye. In order to quantify the Mn^{2+} quench, a sliding average over five adjacent data points (i.e. over 25 s) was calculated; the slope of the curve was obtained by calculating the first time derivative of these data.

The Ca^{2+} concentration within intracellular storing organelles (such as the endoplasmic reticulum) was estimated with the fluorescent dye, Mag-Fura-2 (Molecular Probes) as described previously (Siefjediers *et al.*, 2007). Mag-Fura-2 is a lower affinity Ca^{2+} indicator which is able to measure Ca^{2+} at a concentration of 3 µmol·L^{-1} and higher (Baylor and Hollingworth, 2000). Most of the dye accumulates in the intracellular organelles and little in the cytosol (Hofer and Machen, 1993); its fluorescence at an excitation wavelength of 340 nm increases, when the Ca^{2+} concentration increases. Crypts were incubated for 60 min with 2.5 µmol·L^{-1} Mag-Fura-2 AM.

In order to reveal changes in mitochondrial membrane potential, the fluorescent dye rhodamine 123 was used (Krippeit-Drews *et al.*, 2000). Its fluorescence at an excitation wavelength of 480 nm increases when the mitochondrial membrane potential is depolarized. For these experiments, crypts were incubated for 30 min with 26 µmol·L^{-1} rhodamine 123.

Data analysis

Values are given as means ± SEM. When means of several groups had to be compared, an analysis of variance was performed followed by *post hoc* Tukey's-test. For the comparison of two groups, either a Student's *t*-test or a Mann–Whitney *U*-test was applied. An *F*-test decided which test method had to be used. Both paired and unpaired two-tailed Student's *t*-tests were applied as appropriate. $P < 0.05$ was considered to be statistically significant.

Materials

2′,4′-Dichlorobenzamil hydrochloride (DCB; from Enzo, Lörrach, Germany), glibenclamide, and nystatin were dissolved in dimethylsulphoxide (final maximal concentration 0.5%, v/v). Carbonyl cyanide 4-(trifluoromethoxy) phenylhydrazone (3) (FCCP) was dissolved in ethanol (final concentration 0.01%, v/v). Scilliroside (a generous gift from Sandoz, Basel, Switzerland) was dissolved in methanol (final concentration 0.25%, v/v). Mn^{2+} and tetrapentylammonium (TPeA) were added as chloride salts. If not indicated otherwise, drugs were from Sigma,(Taufkirchen, Germany).

Results

Effect of NaHS on currents across the basolateral membrane

Previous experiments have revealed that NaHS evokes a biphasic Cl^- secretion (interrupted by a negative Isc), which is sensitive to inhibitors of ATP-sensitive and Ca^{2+}-dependent K^+ channels (Hennig and Diener, 2009). In order to study the presumed effects of the H_2S donor on the basolateral membrane, that is, the membrane with the highest cellular K^+ conductance, more directly, the apical membrane was permeabilized by the ionophore, nystatin (100 µg·mL^{-1} at the mucosal side), and a K^+ current across basolateral K^+ channels was driven by a mucosal-to-serosal K^+ gradient (98 mmol·L^{-1} NaCl/13.5 mmol·L^{-1} KCl buffer at the mucosal and 107 mmol·L^{-1} NaCl/4.5 mmol·L^{-1} KCl at the serosal side of the tissue). Baseline Isc prior administration of nystatin amounted 0.64 ± 0.13 µEq·h^{-1}·cm^{-2} (n = 7). In average, nystatin induced a maximal increase

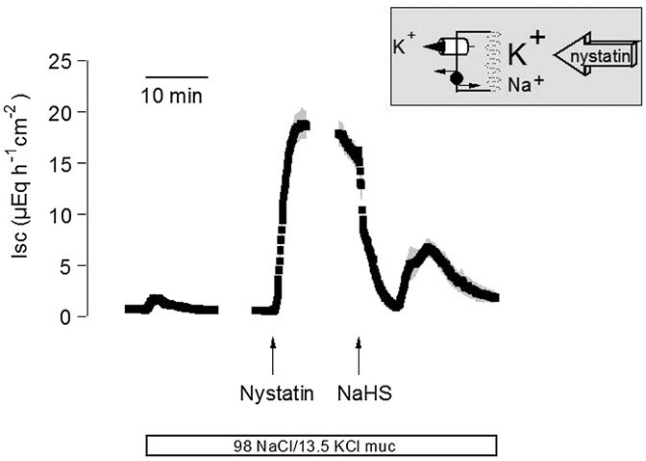

Figure 1

Biphasic change in the overall current across the basolateral membrane evoked by sodium hydrosulphide (NaHS) (10^{-2} mol·L^{-1} at the serosal side; right arrow). The apical membrane was permeabilized with nystatin (100 µg·mL^{-1} at the mucosal side; left arrow). The serosal side was exposed to a 107 mmol·L^{-1} NaCl/4.5 mmol·L^{-1} KCl buffer solution, whereas the mucosal buffer was 98 mmol·L^{-1} NaCl/13.5 mmol·L^{-1} KCl (white bar below trace), so that both basolateral K^+ channels as well as the Na^+-K^+-pump contribute to the nystatin-induced short-circuit current (Isc), as indicated by the schematic inset. Line interruptions are caused by omission of time intervals of 5–10 min in order to synchronize the tracings of individual records to the administration of drugs. Values are given as means (symbols) ± SEM (grey shaded area), n = 7. For statistics, see text.

in Isc to 19.3 ± 1.56 µEq·h^{-1}·cm^{-2} ($P < 0.05$ vs. baseline; Figure 1). Administration of NaHS (10^{-2} mol·L^{-1} at the serosal side) during the plateau phase of the nystatin-induced Isc caused a biphasic change in Isc: an initial decrease followed by a secondary increase (Figure 1). During the decreasing phase of the NaHS response, Isc fell to a value of 0.78 ± 0.14 µEq·h^{-1}·cm^{-2} and increased again to 8.34 ± 0.93 µEq·h^{-1}·cm^{-2} during the secondary phase of the response to the H_2S donor. The concentration of NaHS (10^{-2} mol·L^{-1}) was chosen as a maximal effective concentration from our previous experiments (Hennig and Diener, 2009). A ten times lower concentration of the donor (10^{-3} mol·L^{-1}), which – assuming a yield of NaHS to deliver H_2S of about 30% (Lee *et al.*, 2006) – should result in H_2S concentrations much closer to the plasma concentrations of this gasotransmitter (see Discussion), also resulted in a biphasic change in the current across the basolateral membrane (data not shown). This response, however, exhibited greater variability; so the concentration of 10^{-2} mol·L^{-1} was preferred in order to obtain consistent results.

Under these conditions, two components contribute to the nystatin-induced Isc: a stimulation of the Na^+-K^+-pump (exchanging 3 Na^+ against 2 K^+ with each transport cycle) by the apical inflow of

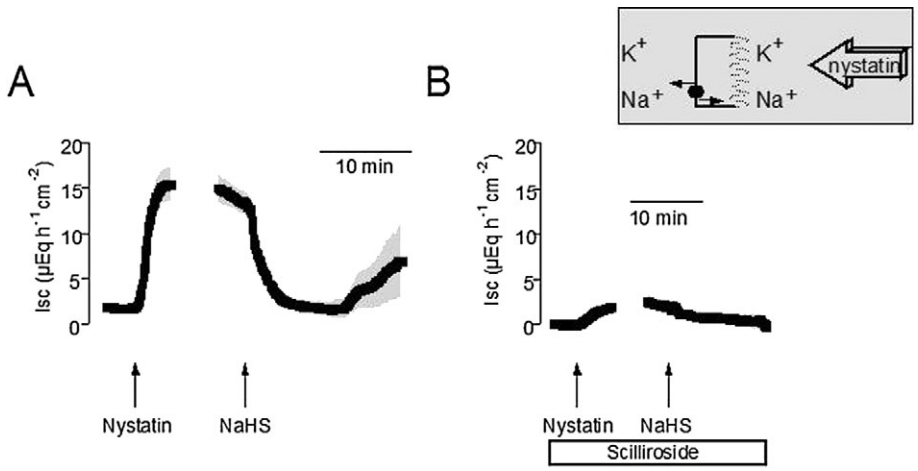

Figure 2

(A) Biphasic change in the current carried by the basolateral Na^+-K^+-pump evoked by sodium hydrosulphide (NaHS) (10^{-2} mol·L^{-1} at the serosal side; right arrow). The apical membrane was permeabilized with nystatin (100 µg·mL^{-1} at the mucosal side; left arrow). The serosal and the mucosal sides were exposed to a 107 mmol·L^{-1} NaCl/4.5 mmol·L^{-1} KCl buffer solution, so that only the Na^+-K^+-pump can contribute to the nystatin-induced short-circuit current (Isc) as indicated by the schematic inset. (B) Scilliroside (10^{-4} mol·L^{-1} at the serosal side; white bar) suppresses the secondary stimulation of pump current by NaHS. Line interruptions are caused by omission of time intervals of 5–10 min in order to synchronize the tracings of individual records to the administration of drugs. Values are given as means (symbols) ± SEM (grey shaded area), n = 8–9. For statistics, see Table 1.

Na^+ via the nystatin pores, and a current across basolateral K^+ channels driven by the applied K^+ gradient (Schultheiss and Diener, 1997). Cation substitution experiments were performed in order to distinguish between these two components. In a first attempt, the current across basolateral K^+ channels was excluded by the omission of a K^+ concentration gradient, that is, the apical membrane was permeabilized in the presence of a 107 mmol·L^{-1} NaCl/4.5 mmol·L^{-1} KCl buffer at both sides of the tissues (Figure 2). Under these conditions, NaHS (10^{-2} mol·L^{-1} at the serosal side) induced a similar, biphasic change in Isc, that is, an initial inhibition of Isc followed by a secondary increase (Figure 2A; for statistics, see Table 1). Pretreatment with scilliroside (10^{-4} mol·L^{-1} at the serosal side), a potent inhibitor of the rat Na^+-K^+-ATPase (Robinson, 1970), strongly inhibited the nystatin-induced Isc under these ionic conditions and suppressed the effect of NaHS (Figure 2B), confirming that this Isc is carried by the basolateral Na^+-K^+-ATPase.

In order to investigate the effects of NaHS on the basolateral K^+ conductance, tissues were permeabilized in the presence of a mucosal-to-serosal K^+ gradient, but in the absence of mucosal Na^+ in order to prevent a contribution of the Na^+-K^+-pump to the measured current (i.e. 98 mmol·L^{-1} NMDGCl/13.5 mmol·L^{-1} KCl buffer at the mucosal and 107 mmol·L^{-1} NaCl/4.5 mmol·L^{-1} KCl at serosal side of the tissue). Again, NaHS (10^{-2} mol·L^{-1} at the serosal side) biphasically modulated the nystatin-induced Isc under these ionic conditions; that is, an initial inhibition was followed by a secondary increase (Figure 3A). Both the nystatin-induced Isc as well as the response to NaHS were significantly

Table 1

Effect of sodium hydrosulphide (NaHS) on currents across the basolateral membrane carried by the Na^+-K^+-pump

	Pump current in the presence of scilliroside Isc (µEq·h^{-1}·cm^{-2})	Pump current without scilliroside Isc (µEq·h^{-1}·cm^{-2})
Baseline	0.00 ± 0.20*	1.74 ± 0.20
Nystatin	2.96 ± 1.03*	16.6 ± 1.82
NaHS decrease	0.11 ± 0.47	1.11 ± 0.64
NaHS peak	2.36 ± 2.41*	9.06 ± 4.57

*P < 0.05 versus Isc in the absence of scilliroside.
Effect of NaHS (10^{-2} mol·L^{-1} at the serosal side) on the current across the basolateral membrane carried by the Na^+-K^+-ATPase in the absence (right) or presence (left) of scilliroside (10^{-4} mol·L^{-1} at the serosal side). The apical membrane was permeabilized with nystatin (100 µg·mL^{-1} at the mucosal side). The serosal and the mucosal side were exposed to a 107 mmol·L^{-1} NaCl/4.5 mmol·L^{-1} KCl buffer solution. The maximal increase in Isc induced by nystatin, the maximal decrease in Isc evoked by NaHS within 20 min after administration of the drug and the maximal increase (peak) evoked by NaHS within 5–20 min after administration of the drug are given. Values are means ± SEM, n = 8–9.
ISC, short-circuit current.

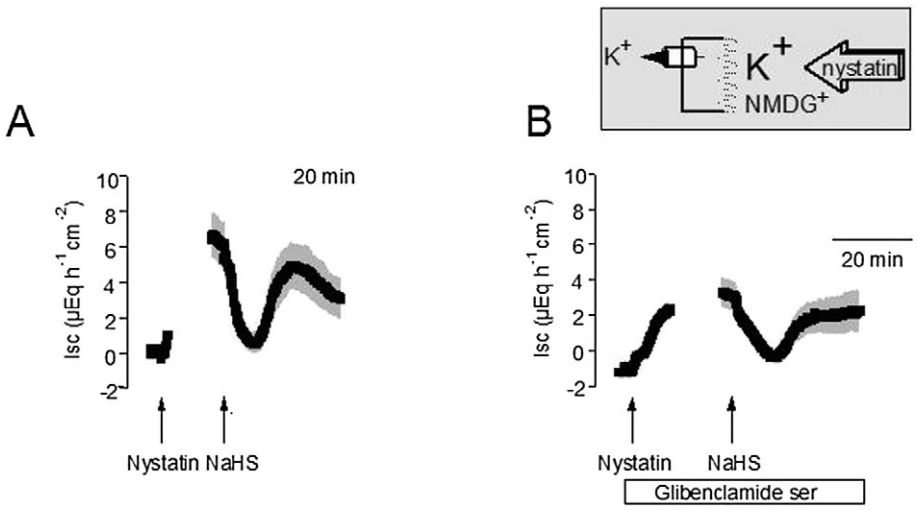

Figure 3

(A) Biphasic change in the current across the basolateral K^+ channels evoked by sodium hydrosulphide (NaHS) (10^{-2} mol·L^{-1} at the serosal side; right arrow). The apical membrane was permeabilized with nystatin (100 µg·mL^{-1} at the mucosal side; left arrow). The serosal side was exposed to a 107 mmol·L^{-1} NaCl/4.5 mmol·L^{-1} KCl buffer solution, whereas the mucosal buffer was a 98 mmol·L^{-1} NMDGCl/13.5 mmol·L^{-1} KCl, so that only basolateral K^+ channels can contribute to the nystatin-induced short-circuit current (Isc) as indicated by the schematic inset. (B) Glibenclamide (10^{-3} mol·L^{-1} at the serosal side; white bar) inhibits the secondary stimulation of Isc by NaHS. Line interruptions are caused by omission of time intervals of 5–10 min in order to synchronize the tracings of individual records to the administration of drugs. Values are given as means (symbols) ± SEM (grey shaded area), n = 6–10. For statistics, see Table 2.

($P < 0.05$) reduced, when the tissues were pretreated with glibenclamide (10^{-3} mol·L^{-1} at the serosal side, Table 2), which acts as a blocker of ATP-sensitive K^+ channels (Figure 3B; see Cook and Quast, 1990).

A further basolateral K^+ conductance, which might be a target of NaHS, is that through Ca^{2+}-dependent K^+ channels, as the H_2S donor induces a biphasic change in the cytosolic Ca^{2+} concentration, that is, an initial fall followed by an increase (Hennig and Diener, 2009). Therefore, tissues were pretreated with TPeA (10^{-4} mol·L^{-1} at the serosal side), a blocker known to inhibit preferentially Ca^{2+}-dependent K^+ channels (Maguire *et al.*, 1999). Under these conditions, nystatin induced only a small increase in K^+ current across the basolateral membrane (Table 3), emphasizing the prominent role of Ca^{2+}-dependent K^+ channels for the overall K^+ conductance of this membrane (Schultheiss and Diener, 1997). When NaHS (10^{-2} mol·L^{-1} at the serosal side) was administered, the typical initial fall in Isc induced by the drug was preserved, whereas the secondary rise in Isc was strongly reduced (Table 3), suggesting that a stimulation of TPeA-sensitive K^+ channels also contributes to this phase of the NaHS response.

Table 2

Effect of sodium hydrosulphide (NaHS) on currents carried by basolateral glibenclamide-sensitive K^+ channels

	Isc (µEq·h^{-1}·cm^{-2}) + glibenclamide	Isc (µEq·h^{-1}·cm^{-2}) – glibenclamide
Baseline	–1.16 ± 0.41*	–0.03 ± 0.26
Nystatin	3.28 ± 0.87*	6.46 ± 1.29
NaHS decrease	–0.40 ± 0.31	0.21 ± 0.54
NaHS peak	2.60 ± 1.12*	6.17 ± 1.30

*$P < 0.05$ versus Isc in the absence of glibenclamide.
Effect of NaHS (10^{-2} mol·L^{-1} at the serosal side) on the current across the basolateral K^+ conductance in the absence (– glibenclamide; right) or presence (+ glibenclamide; left) of glibenclamide (10^{-3} mol·L^{-1} at the serosal side). Tissues were permeabilized with nystatin (100 µg·mL^{-1} at the mucosal side) in the presence of 98 mmol·L^{-1} NMDGCl/13.5 mmol·L^{-1} KCl buffer at the mucosal and 107 mmol·L^{-1} NaCl/4.5 mmol·L^{-1} KCl at the serosal side of the tissue. The maximal increase in Isc induced by nystatin, the maximal decrease in Isc evoked by NaHS within 20 min after administration of the drug and the maximal increase (peak) evoked by NaHS within 5–20 min after administration of the drug are given. Values are means ± SEM, n = 6–10.
ISC, short-circuit current.

Effect of NaHS on mitochondrial membrane potential

The stimulatory effect of H_2S on ATP-sensitive K^+ channels is well known (Zhao *et al.*, 2001; Yang *et al.*, 2005), whereas the initial inhibition of this conductance, as suggested by the glibenclamide-sensitive initial fall in Isc, was unexpected. ATP-sensitive K^+ channels are inhibited by an increase in

Table 3

Effect of sodium hydrosulphide (NaHS) on currents carried by basolateral TPeA-sensitive K^+ channels

	Isc ($\mu Eq \cdot h^{-1} \cdot cm^{-2}$) + TPeA	Isc ($\mu Eq \cdot h^{-1} \cdot cm^{-2}$) – TPeA
Baseline	–1.89 ± 0.62*	1.43 ± 0.19
Nystatin	–1.64 ± 1.02*	6.83 ± 1.29
NaHS decrease	–4.55 ± 1.19*	–0.42 ± 1.04
NaHS peak	–3.81 ± 1.61*	3.27 ± 0.83

*$P < 0.05$ versus Isc in the absence of TPeA.
Effect of NaHS (10^{-2} mol·L^{-1} at the serosal side) on the current across the basolateral K^+ conductance in the absence (– TPeA; right) or presence (+ TPea; left) of tetrapentylammonium (10^{-4} mol·L^{-1} at the serosal side). Tissues were permeabilized with nystatin (100 µg·mL^{-1} at the mucosal side) in the presence of 98 mmol·L^{-1} NNMDGCl/13.5 mmol·L^{-1} KCl buffer at the mucosal and 107 mmol·L^{-1} NaCl/4.5 mmol·L^{-1} KCl at the serosal side of the tissue. The maximal increase in Isc induced by nystatin, the maximal decrease in Isc evoked by NaHS within 20 min after administration of the drug and the maximal increase (peak) evoked by NaHS within 5–20 min after administration of the drug are given. Values are means ± SEM, $n = 7–8$.
ISC, short-circuit current; TPeA, tetrapentylammonium.

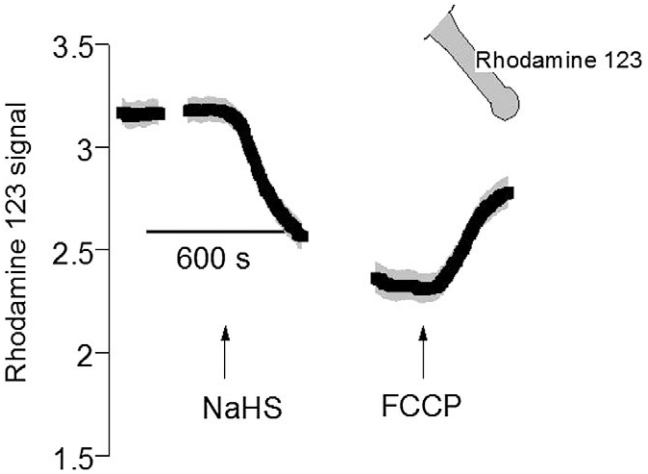

Figure 4

Hyperpolarization of the mitochondrial membrane potential by sodium hydrosulphide (NaHS) (10^{-4} mol·L^{-1}; left arrow). Isolated colonic crypts were loaded with rhodamine 123 as indicated by the inset. At the end of the experiment, Carbonyl cyanide 4-(trifluoromethoxy) phenylhydrazone (3) (FCCP; 10^{-6} mol·L^{-1}; right arrow) was administered. The rhodamine 123 fluorescence is given in arbitrary units. Line interruptions are caused by omission of time intervals of 5–10 min in order to synchronize the tracings of individual records to the administration of drugs. Values are given as means (symbols) ± SEM (grey shaded area), $n = 89$. For statistics, see text.

the cytosolic ATP concentration (Seino and Miki, 2003). The rate of ATP synthesis is strongly dependent on mitochondrial membrane potential (Duchen *et al.*, 1993); a high rate of ATP synthesis depolarizes the mitochondrial membrane potential due to the reduction of the H^+ gradient (Garlid and Paucek, 2003).

Therefore, in order to (indirectly) estimate whether this dual action of NaHS might be related to alterations in the cellular ATP production, changes in mitochondrial membrane potential were measured with the fluorescent dye, rhodamine 123, whose signal is quenched by this potential. For these experiments, isolated colonic crypts were used, which in our previous study (Hennig and Diener, 2009) had shown to be much more sensitive to NaHS compared with the thick mucosa–submucosa preparations used in the Ussing chamber. Therefore, the NaHS concentration was reduced to 10^{-4} mol·L^{-1}. However, in contrast to the expectation of a mitochondrial depolarization, which should result from an increase in ATP synthesis, the administration of NaHS caused a prompt decrease of the rhodamine 123 signal from 3.18 ± 0.061 to 2.34 ± 0.078 arbitrary units ($P < 0.05$, $n = 89$; Figure 4), that is, a hyperpolarization. As a control, the uncoupler of the oxidative phosphorylation, FCCP (10^{-6} mol·L^{-1}), was administered, which – as expected – caused an increase in the rhodamine 123 fluorescent signal to 2.84 ± 0.076 arbitrary units ($P < 0.05$ vs. the signal in the presence of NaHS). Consequently, it seems unlikely that the unconventional inhibition of ATP-sensitive basolateral K^+ conductance, which is finally superimposed by the expected stimulation due to direct interaction of H_2S with the channel molecules (Figure 3), might be caused by an increase in the cytosolic ATP level, although this conclusion remains speculative without determination of the cytosolic ATP concentration.

Effect of intracellular Ca^{2+}

In previous experiments (see also Figure 7B of the present study), we observed that NaHS induces a biphasic change in the cytosolic Ca^{2+} concentration, that is, an initial fall followed by a secondary increase mediated by a release of stored Ca^{2+}, mainly via ryanodine receptors (Hennig and Diener, 2009). As such a change in the cytosolic Ca^{2+} concentration would also affect the basolateral K^+ conductance via modulation of Ca^{2+}-dependent K^+ channels, we tried to find out, which mechanism might underlie the initial fall in $[Ca^{2+}]_i$, which is still completely unexplained.

In a first attempt, we asked the question whether an uptake of Ca^{2+} into Ca^{2+}-storing organelles such as the endoplasmic reticulum might be involved in the early NaHS response. However, NaHS did not affect, at all, the fluorescence signal of Mag-Fura-2, a

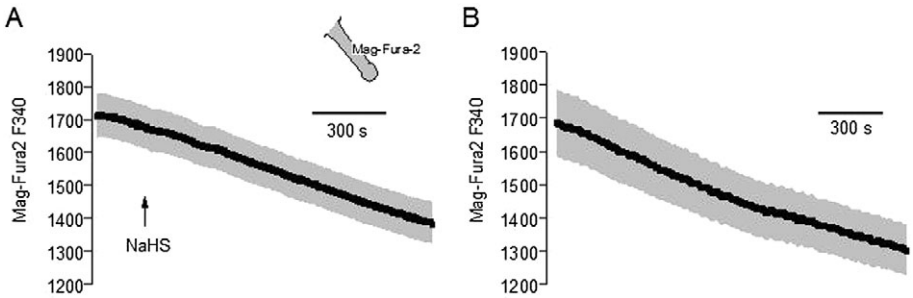

Figure 5

(A) Sodium hydrosulphide (NaHS) (10^{-4} mol·L^{-1}; arrow) does not affect the Mag-Fura-2 emission (in arbitrary units) at an excitation wavelength of 340 nm (F 340 nm, i.e. the wavelength where the dye exhibits the strongest change in fluorescence in response to changes in the Ca^{2+} concentration). (B) Time-dependent control without administration of NaHS. Isolated crypts were loaded with Mag-Fura-2 (as indicated by the inset). Values are given as means (symbols) ± SEM (grey shaded area), n = 96–97.

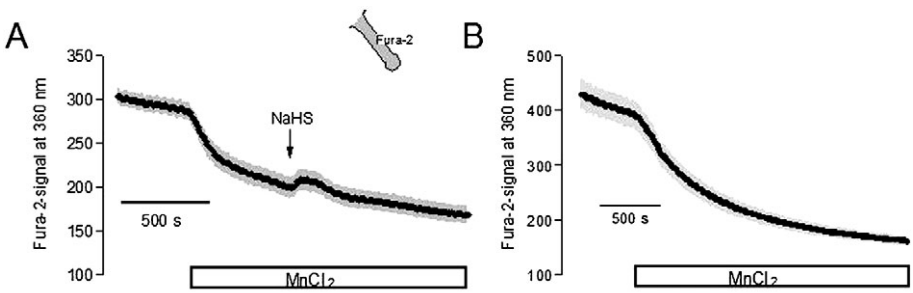

Figure 6

(A) Mn^{2+} (5 10^{-4} mol·L^{-1} $MnCl_2$; white bar) leads to a decrease in the Fura-2 signal (in arbitrary units) measured at an excitation wavelength of 360 nm (at which the Fura-2 signal is independent from the cytosolic Ca^{2+} concentration) at isolated colonic crypts (indicated by the schematic). The administration of sodium hydrosulphide (NaHS) (10^{-4} mol·L^{-1}; arrow) transiently reverses the Mn^{2+} quench, suggesting a stimulation of Ca^{2+} (Mn^{2+}) efflux by NaHS. For statistics, see text. (B) Time-dependent control without administration of NaHS. Values are given as means (symbols) ± SEM (grey shaded area) of n = 12 cells measured synchronously.

fluorescent dye, which accumulates in intracellular Ca^{2+} stores (Figure 5A; see Hofer and Machen, 1993); there was only a continuous fall in the Mag-Fura-2 signal, which was also observed in time-dependent control experiments (Figure 5B).

Consequently, the fall in the cytosolic Ca^{2+} concentration should be caused by a stimulation of Ca^{2+} efflux. To test this hypothesis, the following approach was used. The fluorescence of Fura-2 is quenched by Mn^{2+}. Mn^{2+} ions are accepted as substrate by many Ca^{2+}-transporting proteins (see Parekh and Penner, 1997; Trepakova *et al.*, 1999) and lead, once within the cell, to a quench of the Fura-2 fluorescence. When the Fura-2 fluorescence was measured at an excitation wave length of 360 nm, that is, at the isoemissive wave length, where the signal is not affected by the cytosolic Ca^{2+} concentration, the administration of Mn^{2+} (5 10^{-4} mol·L^{-1}) caused a prompt fall in the Fura-2 fluorescence signal (Figure 6). When subsequently NaHS (10^{-4} mol·L^{-1}) was administered, it caused a transient increase in the Fura-2 signal (Figure 6A), which was not observed in time-dependent control experiments (Figure 6B). The slope, by which the Fura-2 signal changed, amounted to –3.31 ± 0.27 units/5 s before and 4.27 ± 0.51 units/5 s (P < 0.05 vs. slope in the absence of NaHS, n = 84) during the steepest phase of the NaHS response. In contrast, in parallel-performed time-dependent control experiments, where no NaHS was administered, the maximal change in the Fura-2 slope only amounted to 0.79 ± 0.20 units/5 s (P < 0.05 vs. effect of NaHS, n = 72). Consequently, NaHS transiently activates a Ca^{2+} (Mn^{2+}) efflux pathway.

One prominent Ca^{2+} extruding mechanism at rat colonic crypts is a Na^+-Ca^{2+}-exchanger (Seip *et al.*, 2001). Therefore, in a final set of experiments, we tested whether a stimulation of this exchanger might be responsible for the transient fall in the cytosolic Ca^{2+} concentration induced by NaHS. When NaHS (10^{-4} mol·L^{-1}) was administered in the presence of dichlorobenzamil (2.5 10^{-6} mol·L^{-1}), a

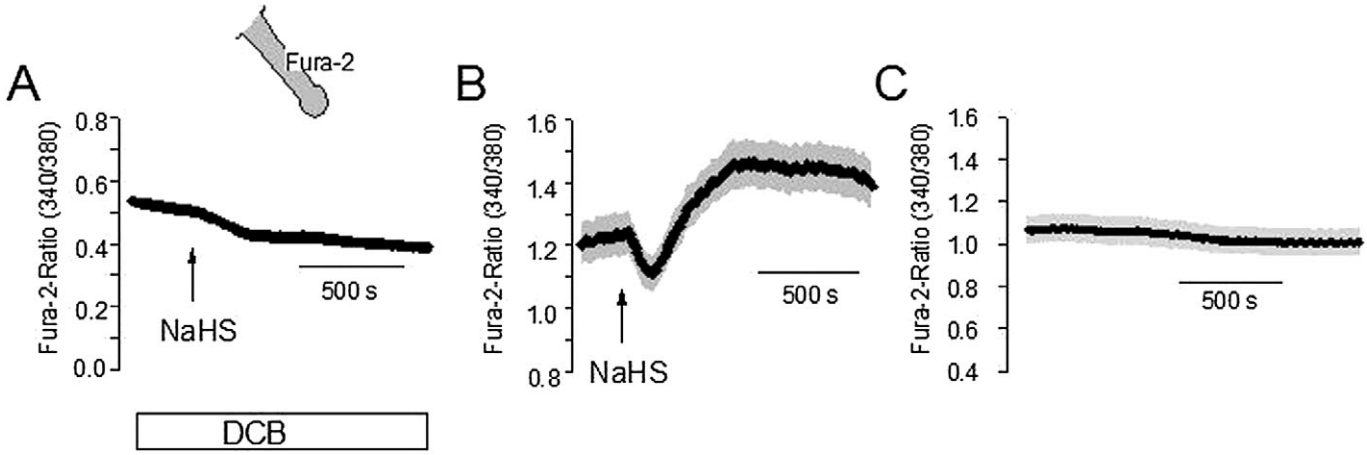

Figure 7

(A) Pretreatment with 2′,4′-dichlorobenzamil (DCB; $2.5.10^{-6}$ mol·L^{-1}; white bar) prevents the changes in the Fura-2 ratio evoked by sodium hydrosulphide (NaHS) (10^{-4} mol·L^{-1}; arrow) in comparison with control crypts not pretreated with DCB (B). (C) Time-dependent control without administration of NaHS. Isolated crypts were loaded with Fura-2 (as indicated by the schematic); given is the emission at an excitation wavelength of 340 nm divided by the emission at an excitation wave length of 380 nm. Values are given as means (symbols) ± SEM (grey shaded area), n = 52–84. For statistics, see Table 4.

Table 4

Effect of sodium hydrosulphide (NaHS) on the cytosolic Ca^{2+} concentration

	Δ Fura-2 ratio Initial decrease	Δ Fura-2 ratio Secondary peak
+ DCB	–0.0577 ± 0.00416*	–0.0071 ± 0.00103*
– DCB	–0.200 ± 0.0240	0.370 ± 0.0446
NMDG Cl	–0.0542 ± 0.00696*	0.0842 ± 0.00965*
NaCl	–0.131 ± 0.0203	0.247 ± 0.0471

*P < 0.05 versus response to NaHS under control conditions (i.e. without DCB or in the presence of Na^+ respectively).
Effect of NaHS (10^{-4} mol·L^{-1}) on the Fura-2 signal in the presence (+ DCB) or absence (– DCB) of DCB ($2.5.10^{-4}$ mol·L^{-1}; upper two rows), or in the absence (NMDG Cl) or presence (NaCl) of extracellular Na^+ (lower two rows). The initial decrease (middle column) was calculated as the minimum signal reached within 4 min after administration of NaHS (10^{-4} mol·L^{-1}), whereas the secondary increase (right column) was calculated as maximum within 15 min after administration of NaHS. Data are given as change in the Fura-2 ratio (Δ Fura-2 ratio) compared with the baseline just prior to administration of NaHS and are means ± SEM, n = 52–83.
DCB, 2′,4′-dichlorobenzamil.

known inhibitor of this exchanger (see Seip *et al.*, 2001), the effect of the H_2S donor was drastically reduced (Figure 7A,B, Table 4), whereas in time-dependent control experiments a stable baseline of the Fura-2 ratio signal was measured (Figure 7C). Surprisingly, both the initial decrease as well as the secondary increase of the cytosolic Ca^{2+} concentration were inhibited, which might suggest non-specific actions of DCB on transporters other than the Na^+-Ca^{2+}-exchanger. However, when a different approach was used to inhibit the Ca^{2+} extruding action of the exchanger, that is, when the crypts were superfused with a Na^+-free solution, a similar inhibition of both phases of the NaHS response was observed (Table 4).

Discussion

In the intestine, the gaso-transmitter H_2S is known to exert several actions such as a relaxation of smooth muscle from different species (Teague *et al.*, 2002), antinociceptive (Distrutti *et al.*, 2006) or anti-inflammatory effects (Fiorucci *et al.*, 2007). A further prominent action is the induction of anion secretion (Schicho *et al.*, 2006). This anion secretion leads to an increase in Isc across the epithelium. Two phases of the Isc increase induced by the H_2S donor, NaHS, can be distinguished in rat colonic epithelium: an early one, transiently interrupted by a fall in Isc, before the current increases again to reach a long-lasting plateau (Hennig and Diener, 2009). The present data suggest that, at the basolateral membrane, three sites of action are involved in the complex Isc pattern evoked by NaHS, that is: (i) the basolateral Na^+-K^+-ATPase; (ii) glibenclamide-sensitive, ATP-sensitive K^+ channels; and (iii) TPeA-sensitive, Ca^{2+}-dependent K^+ channels.

One action of the H_2S donor, NaHS, consists in a biphasic modulation of the current across the basolateral membrane carried by the Na^+-K^+-ATPase in

apically permeabilized epithelia (Figure 2A). A transient inhibition is followed by a secondary increase in pump current. In order to confirm that this current is indeed caused by this enzyme, scilliroside was used, as the α_1-isoform of the Na^+-K^+-ATPase in rats is quite resistant to the classical Na^+-K^+-pump inhibitor, ouabain (see Edwards and Pallone, 2007). Pretreatment with this potent inhibitor of the rat Na^+-K^+-ATPase (Robinson, 1970) suppressed the action of NaHS (Figure 2B). Consequently, there seems to be a biphasic modulation by H_2S of the pump activity, which finally maintains the K^+ concentration gradient at the cell membrane and thereby sets the fundamental driving force for active ion transport. The mechanism of this modulation is not known, but it is tempting to speculate that this action may be related to a reduction of disulphide bonds within the protein by H_2S, which acts as reducing agent (Reiffenstein *et al.*, 1992), or a modification of free thiol groups. However, the Isc response evoked by NaHS at rat distal colon was not inhibited by the pretreatment of the tissue with N-ethylmaleimide (NEM; $5{\cdot}10^{-5}$ mol·L^{-1}, unpublished data), a drug assumed to block non-protein SH-groups (Chávez-Pińa *et al.*, 2010), suggesting that the latter explanation is less probable.

Another site of action of H_2S in the basolateral membrane is the glibenclamide-sensitive K^+ channel (Figure 3) and such channels are considered to be classical targets of H_2S. An increase in this type of cellular K^+ conductance is known from vascular smooth muscle cells and is assumed to be mediated by a reduction of disulphide bonds within the channel protein (Zhao *et al.*, 2001). Obviously, an increase in the open probability of the channels is responsible for this response as observed in a rat insulinoma cell line (Yang *et al.*, 2005). ATP-sensitive K^+ channels serve to couple membrane potential to the metabolic state of the cell. They are octomers, composed of four channel-forming subunits ($K_{IR}6.1$ or $K_{IR}2$) and four regulatory subunits, the sulphonylurea receptors (SUR1, SUR2A or SUR2B; see Seino and Miki, 2003). Immunohistochemically, $K_{IR}6.1$ and SUR2A have been found in human and rat small intestinal epithelium (Jöns *et al.*, 2006). Basolateral administration of a K^+ channel opener such as pincacidil, which stimulates ATP-sensitive K^+ channels, evokes an increase in Isc across rat colon (Hennig and Diener, 2009), suggesting the presence of this type of cation channel in the rat colonic epithelium, although molecular or immunohistochemical evidence is still missing. Surprisingly, the effect of NaHS on the current carried by ATP-sensitive K^+ channels was also biphasic: that is, the expected activation was preceded by a transient inhibition (Figure 3).

ATP-sensitive K^+ channels are inhibited by an increase in the cytosolic concentration of ATP, which binds to the regulatory nucleotide binding site of the respective SUR subunits (Seino and Miki, 2003), so it might be hypothesized that the paradoxical, transient inhibition of the glibenclamide ATP-sensitive K^+ conductance might be caused by an increase in the ATP concentration within the cell. A high rate of ATP synthesis is known to depolarize the mitochondrial membrane potential due to the reduction of the H^+ gradient (Garlid and Paucek, 2003). However, the fluorescence signal of the fluorescent dye, rhodamine 123, which incorporates into the inner mitochondrial membrane and whose fluorescence is quenched by this potential, was reduced (and not enhanced) by NaHS, whereas a typical uncoupler of phosphorylation such as FCCP, a protonophore, which dissipates the H^+ gradient at this membrane, evoked the opposite signal (Figure 4). H_2S is known to inhibit mitochondrial respiration, probably at the level of the cytochrome C oxidase, that is, the complex IV of the mitochondrial electron transport chain; this action is thought to be the reason for the protective effect of H_2S on the myocardium after ischemia/reperfusion damage (Elrod *et al.*, 2007). This inhibition probably underlies the observed hyperpolarization of the inner mitochondrial membrane (Figure 4). Consequently, the unexpected inhibition of ATP-sensitive basolateral K^+ conductance, finally superimposed by the expected stimulation (Figure 3), is probably not related to an increase in the cytosolic ATP level, at least not on the level of the mitochondrial ATP production. Alternatively, a reduction in ATP degradation, for example, by the transient reduction in Na^+-K^+-pump activity, might cause an increase in the local concentration of ATP near the basolateral membrane and thereby transiently inhibit ATP-sensitive K^+ channels.

At first glance, an alternative explanation for the hyperpolarizing action of H_2S at the mitochondrial membrane potential might be thought. ATP-sensitive K^+ channels are also found in the inner mitochondrial membrane (Inoue *et al.*, 1991); as found with their counterparts in the cell membrane, they might also be activated by H_2S, too. However, as the K^+ concentration in the mitochondrial matrix and in the inter-membrane space are approximately equal (Garlid and Paucek, 2003), their activation would tend to depolarize the inner mitochondrial membrane.

In the basolateral membrane, apart from the ATP-sensitive K^+ conductance, the dominant Ca^{2+}-dependent K^+ conductance was also modulated in a biphasic manner by NaHS (Table 3). This response is paralleled by changes in the cytosolic Ca^{2+}

concentration (Figure 7B): a transient fall, which will lead to a decrease of basolateral K^+ conductance, and a secondary rise, which will then increase the basolateral K^+ conductance. The mechanism of the secondary increase has recently been shown to be independent from extracellular Ca^{2+}, but related to a release of Ca^{2+} from intracellular Ca^{2+} storing organelles via ryanodine receptors (Hennig and Diener, 2009), which are expressed by rat colonic epithelium (Prinz and Diener, 2008). In the present study, we focused on the pathways involved in the initial fall of the cytosolic Ca^{2+} concentration induced by the NaHS. The administration of NaHS to isolated colonic crypts transiently reversed the quench of the Fura-2 signal induced by Mn^{2+} (Figure 6A). Mn^{2+} ions are substrates for many Ca^{2+} transporters and reduce, once within the cytoplasm, the Fura-2 signal (cf. the rapid fall of the Fura-2 fluorescence in Figure 6). Consequently, these data suggest a transient stimulation of Ca^{2+} (Mn^{2+}) outflow by NaHS. The change in the cytosolic Ca^{2+} concentration could be inhibited by two different strategies to inhibit the Na^+-Ca^{2+}-exchanger in the cell membrane. Both DCB, a blocker of this exchanger (Seip *et al.*, 2001), as well as the substitution of Na^+ by the impermeant cation, $NMDG^+$, inhibited the action of NaHS on the Fura-2 signal (Figure 7A, Table 4), suggesting a transient stimulation of Na^+-Ca^{2+}-exchange by H_2S.

Another possible pathway to decrease the cytosolic Ca^{2+} concentration is the sequestration of Ca^{2+} into intracellular Ca^{2+} storing organelles such as the endoplasmic reticulum. However, the fluorescence signal of Mag-Fura-2, a low Ca^{2+} affinity fluorescent dye which accumulates in these organelles, was unaltered by NaHS (Figure 5). However, it might be possible that a part of the cytosolic Ca^{2+} is taken up into the mitochondria due to the observed hyperpolarization (Figure 4), which would in addition contribute to the decrease in the cytosolic Ca^{2+} level.

These observations about the mechanism of the prosecretory action of H_2S differ from the data obtained from guinea pig and human colon, where neuronal capsaicin-sensitive cation (TRPV1) channels are thought to be the primary target of H_2S (Schicho *et al.*, 2006). In these tissues, H_2S excites afferent nerves (shown with extracellular recordings) that are thought to release substance P, which finally leads to the activation of cholinergic secretomotor neurons as shown by experiments with specific inhibitors (Krueger *et al.*, 2010). Also in rat colon, a part of the secretory response evoked by NaHS is inhibited by the neurotoxin, tetrodotoxin (Hennig and Diener, 2009), but there is a clear epithelial component, as can be seen from the increase in the cytosolic Ca^{2+} concentration of isolated colonic crypts free of any neuronal cells. The reason for this discrepancy is unclear, but may of course represent species difference. On the other hand, we used a relatively high concentration (10^{-2} mol·L^{-1}) of NaHS, which should result in H_2S concentrations even higher than in the colonic lumen, which are estimated to be in the range of up to 10^{-3} mol·L^{-1} (Krueger *et al.*, 2010), in order to obtain a consistent induction of all phases of the Isc response (see Results). Thus, there is the possibility that a high concentration of 10^{-2} mol·L^{-1} NaHS might – in addition to the clear neuronal effects –also stimulate tetrodotoxin-resistant responses in human or guinea pig colon.

What are the functional implications of the present results? H_2S is considered as a gaseous neurotransmitter used by enteric neurons to modulate gastrointestinal functions (Schicho *et al.*, 2006; Krueger *et al.*, 2010). As shown here, this gasotransmitter affects key processes for ion transport within the epithelium such as the cytosolic Ca^{2+} concentration, the activity of the Na^+-K^+-pump, that is, the 'motor' for all active transport processes, as well as the cellular K^+ conductance, which determines the height of the membrane potential. Furthermore, organosulphur compounds from dietary compounds such as garlic are known to be converted to H_2S in a glutathione-dependent manner inside the body; this may be the reason for the cardioprotective effect of garlic (Benavides *et al.*, 2007). If this process is to start during intestinal absorption, it is possible that organosulphur compounds could also exert actions on the intestinal epithelium, such as protective action against ischaemic damage due to the observed mitochondrial hyperpolarization (Figure 4). A further potential source of H_2S *in vivo* is sulphate-reducing bacteria (such as *Desulfovibrio* or *Desulfomonas* species). They are able to reduce SO_4^{2-}, contained in food or in intestinal secretions, to sulphides including H_2S (Florin *et al.*, 1991), and thereby contribute to a permanent exposure of the epithelium, especially of the colon, to H_2S, with its pronounced effects on epithelial ion transport. Plasma levels of H_2S have been reported in the range of 50–160 10^{-6} mol·L^{-1} (Zhao *et al.*, 2003). The local concentration in the vicinity of the intestinal epithelium is unknown, but the production rate has been measured for rat ileum to be in the range of 12 10^{-9} mol·min^{-1}·g^{-1} tissue (Zhao *et al.*, 2003). It has been reported that patients with ulcerative colitis have an increased number of sulphate-reducing bacteria (Roediger *et al.*, 1993), which produce sulphides including H_2S from SO_4^{2-} in the diet or S-containing amino acids. Consequently, the ability of H_2S to modulate basolateral K^+ channels and

thereby determine the driving force for epithelial secretion may also play a role in the pathogenesis of gastrointestinal diseases.

Acknowledgements

The diligent care of Mrs B. Brück, E. Haas, B. Schmitt and A. Stockinger is a pleasure to acknowledge. This study is supported by Deutsche Forschungsgemeinschaft, grant Di 388/11-1.

Conflict of interest

The authors state no conflict of interest.

References

Alexander SPH, Mathie A, Peters JA (2009). Guide to receptors and channels (GRAC), 4th edn. Br J Pharmacol 158 (Suppl. 1): S1–S254.

Baylor SM, Hollingworth S (2000). Measurement and interpretation of cytoplasmic [Ca^{2+}] signals from calcium-indicator dyes. News Physiol Sci 15: 19–26.

Benavides GA, Squadrito GL, Mills RW, Patel HD, Isbell TS, Patel RP *et al*. (2007). Hydrogen sulfide mediates the vasoactivity of garlic. Proc Natl Acad Sci USA 104: 17977–17982.

Binder HJ, Sandle GJ (1994). Electrolyte transport in the mammalian colon. In: Johnson LR (ed.). Physiology of the Gastrointestinal Tract, 3rd edn. Raven Press: New York, pp. 2133–2171.

Chávez-Piña AE, Tapia-Alvarez GR, Navarrete A (2010). Inhibition of endogenous hydrogen sulfide synthesis by PAG protects against ethanol-induced gastric damage in the rat. Eur J Pharmacol 630: 131–136.

Cook NS, Quast U (1990). Potassium channels. Structure, classification, function and therapeutic potential. In: Cook NS (ed.). Potassium Channel Pharmacology. Ellis Horwood: New York, pp. 181–255.

Distrutti E, Sediari L, Mencarelli A, Renga B, Orlandi S, Antonelli E *et al*. (2006). Evidence that hydrogen sulfide exerts antinociceptive effects in the gastrointestinal tract by activating K_{ATP} channels. J Pharmacol Exp Ther 316: 325–335.

Duchen MR, Smith PA, Ashcroft FM (1993). Substrate-dependent changes in mitochondrial function, intracellular free calcium concentration and membrane channels in pancreatic β-cells. Biochem J 294: 35–42.

Edwards A, Pallone TL (2007). Ouabain modulation of cellular calcium stores and signaling. Am J Physiol Renal Physiol 293: F1518–F1532.

Ekundi-Valentim E, Santos KT, Camargo EA, Denadai-Souza A, Teixeira SA, Zanoni CI *et al*. (2010). Differing effects of exogenous and endogenous hydrogen sulphide in carrageenan-induced knee joint synovitis in the rat. Br J Pharmacol 159: 1463–1474.

Elrod JW, Calvert JW, Morrison J, Doeller JE, Kraus DW, Tao L *et al*. (2007). Hydrogen sulfide attenuates myocardial ischemia-reperfusion injury by preservation of mitochondrial function. Proc Natl Acad Sci USA 104: 15560–15565.

Esechie A, Enkhbaatar P, Traber DL, Jonkam C, Lange M, Hamahata A *et al*. (2009). Beneficial effect of a hydrogen sulphide donor (sodium sulphide) in an ovine model of burn- and smoke-induced acute lung injury. Br J Pharmacol 158: 1442–1453.

Fiorucci S, Orlandi S, Mencarelli A, Caliendo G, Santagada V, Distrutti E *et al*. (2007). Enhanced activity of a hydrogen sulphide-releasing derivative of mesalamine (ATB-429) in a mouse model of colitis. Br J Pharmacol 150: 996–1002.

Florin T, Neale G, Gibson GR, Christl SU, Cummings JK (1991). Metabolism of dietary sulphate: absorption and excretion in humans. Gut 32: 766–773.

Garlid KD, Paucek P (2003). Mitochondrial potassium transport: the K^+ cycle. Biochim Biophys Acta 1606: 23–41.

Geng B, Cui YY, Zhao J, Yu F, Zhu Y, Xu G *et al*. (2007). Hydrogen sulfide downregulates the aortic L-arginine/nitric oxide pathway in rats. Am J Physiol Regul Integr Comp Physiol 293: R1608–R1618.

Grynkiewicz G, Poenie M, Tsien RY (1985). A new generation of Ca^{2+} indicators with greatly improved fluorescence properties. J Biol Chem 260: 3440–3450.

Hennig B, Diener M (2009). Actions of hydrogen sulfide on ion transport across rat distal colon. Br J Pharmacol 158: 1263–1275.

Hofer AM, Machen TE (1993). Technique for in situ measurement of calcium in intracellular inositol 1,4,5-trisphophate-sensitive stores using the fluorescent indicator Mag-Fura-2. Proc Natl Acad Sci USA 90: 2598–2602.

Inoue I, Nagase H, Kishi K, Higuti T (1991). ATP-sensitive K^+ channel in the mitochondrial inner membrane. Nature 352: 244–247.

Jöns T, Wittschieber D, Beyer A, Meier C, Brune A, Thomzig A *et al*. (2006). K^+-ATP-channel-related protein complexes: potential transducers in the regulation of epithelial tight junction permeability. J Cell Sci 119: 3087–3097.

Krippeit-Drews P, Dufer M, Drews G (2000). Parallel oscillations of intracellular calcium activity and mitochondrial membrane potential in mouse pancreatic B-cells. Biochem Biophys Res Commun 267: 179–183.

Krueger D, Foerster M, Mueller K, Zeller F, Slotta-Huspenina J, Donovan J *et al*. (2010). Signaling mechanisms involved in the intestinal pro-secretory

actions of hydrogen sulfide. Neurogastroenterol Motil doi: 10.1111/j.1365-2982.2010.01571.x.

Lee SW, Hu YS, Hu LF, Lu Q, Dawe GS, Moore PK *et al.* (2006). Hydrogen sulphide regulates calcium homeostasis in microglial cells. Glia 54: 116–124.

Lefer DJ (2008). Potential importance of alterations in hydrogen sulphide (H_2S) bioavailability in diabetes. Br J Pharmacol 155: 617–619.

Lindström CG, Rosengren JE, Fork FT (1979). Colon of the rat. An anatomic, histologic and radiographic investigation. Acta Radiol Diagn 20: 523–536.

Maguire D, MacNamara B, Cuffe JE, Winter D, Doolan CM, Urbach V *et al.* (1999). Rapid responses to aldosterone in human distal colon. Steroids 64: 51–63.

Parekh AB, Penner R (1997). Store depletion and calcium influx. Physiol Rev 77: 901–930.

Prinz G, Diener M (2008). Characterization of ryanodine receptors in the rat colonic epithelium. Acta Physiol 193: 151–162.

Reiffenstein RJ, Hulbert WC, Roth SH (1992). Toxicology of hydrogen sulfide. Annu Rev Pharmacol Toxicol 1992: 109–134.

Robinson JWL (1970). The difference in sensitivity to cardiac steroids of (Na^+-K^+)-stimulated ATPase and amino acid transport in the intestinal mucosa of the rat and other species. J Physiol 206: 41–60.

Roediger WEW, Duncan A, Kapaniris O, Millard S (1993). Sulphide impairment of substrate oxidation in rat colonocytes: a biochemical basis for ulcerative colitis? Clin Sci 85: 623–627.

Schicho R, Krueger D, Zeller F, von Weyhern CWH, Frieling T, Kimura H *et al.* (2006). Hydrogen sulfide is a novel prosecretory neuromodulator in the guinea-pig and human colon. Gastroenterology 131: 1542–1552.

Schultheiss G, Diener M (1997). Regulation of apical and basolateral K^+ conductances in the rat colon. Br J Pharmacol 122: 87–94.

Schultheiss G, Kocks SL, Diener M (2002). Methods for study of ionic currents and Ca^{2+} signals in isolated colonic crypts. Biol Proced Online 3: 70–78.

Seino S, Miki T (2003). Physiological and pathophysiological roles of ATP-sensitive K^+ channels. Prog Biophys Mol Biol 81: 133–176.

Seip G, Schultheiss G, Kocks SL, Diener M (2001). Interaction between store-operated nonselective cation channels and Na^+-Ca^{2+}-exchanger during secretion in the rat colon. Exp Physiol 86: 461–468.

Siefjediers A, Hardt M, Prinz G, Diener M (2007). Characterization of inositol 1,4,5-trisphosphate (IP_3) receptor subtypes at rat colonic epithelium. Cell Calcium 41: 303–315.

Strabel D, Diener M (1995). Evidence against direct activation of chloride secretion by carbachol in the rat distal colon. Eur J Pharmacol 274: 181–191.

Teague B, Asiedu S, Moore PK (2002). The smooth muscle relaxant effect of hydrogen sulphide in vitro: evidence for a physiological role to control intestinal contractility. Br J Pharmacol 137: 139–145.

Trepakova ES, Cohen RA, Bolotina VM (1999). Nitric oxide inhibits capacitative cation influx in human platelets by promoting sarcoplasmic/endoplasmic reticulum Ca^{2+}-ATPase-dependent refilling of Ca^{2+} stores. Circulation Res 84: 201–209.

Wang R (2002). Two's company, three's a crowd: can H_2S be the third endogenous gaseous transmitter? FASEB J 16: 1792–1798.

Warth R, Barhanin J (2003). Function of K^+ channels in the intestinal epithelium. J Membr Biol 193: 67–78.

Yang W, Yang G, Jia X, Wu L, Wang R (2005). Activation of K_{ATP} channels by H_2S in rat insulin-secreting cells and the underlying mechanisms. J Physiol 569: 519–531.

Zhao W, Zhang J, Lu Y, Wang R (2001). The vasorelaxant effect of H_2S as a novel endogenous gaseous K_{ATP} channel opener. EMBO J 20: 6008–6016.

Zhao W, Ndisang JS, Wang R (2003). Modulation of endogenous production of H_2S in rat tissues. Can J Physiol Pharmacol 81: 848–853.